Activation of Tel1^{ATM} kinase requires Rad50 ATPase and long nucleosome-free DNA but no DNA ends

Received for publication, March 12, 2019, and in revised form, May 7, 2019 Published, Papers in Press, May 9, 2019, DOI 10.1074/jbc.RA119.008410

Sarem Hailemariam[‡], **Sandeep Kumar**[‡1], **and Peter M. Burgers**[‡2]

From the Department of Biochemistry and Molecular Biophysics, Washington University School of Medicine, St. Louis, Missouri 63110

Edited by Patrick Sung

In *Saccharomyces cerevisiae*, Tel1 protein kinase, the ortholog of human ataxia telangiectasia–mutated (ATM), is activated in response to DNA double-strand breaks. Biochemical studies with human ATM and genetic studies in yeast suggest that recruitment and activation of Tel1^{ATM} depends on the heterotrimeric MRX^{MRN} complex, composed of Mre11, Rad50, and Xrs2 (human Nbs1). However, the mechanism of activation of Tel1 by MRX remains unclear, as does the role of effector DNA. Here we demonstrate that dsDNA and MRX activate Tel1 synergistically. Although minimal activation was observed with 80-mer duplex DNA, the optimal effector for Tel1 activation is long, nucleosome-free DNA. However, there is no requirement for DNA double-stranded termini. The ATPase activity of Rad50 is critical for activation. In addition to DNA and Rad50, either Mre11 or Xrs2, but not both, is also required. Each of the three MRX subunits shows a physical association with Tel1. Our study provides a model of how the individual subunits of MRX and DNA regulate Tel1 kinase activity.

Genome stability mechanisms are essential for the normal function of cells. Genomic integrity can be disrupted because of errors caused during DNA replication and by both endogenous and exogenous DNA-damaging agents. Double-strand breaks (DSBs)[3] are among the most cytotoxic and deleterious forms of DNA lesions. The efficient repair of DSBs is essential for genome integrity. DSBs can be formed by exogenous agents, but they can also occur during normal cellular processes, such as during meiosis, immunoglobulin gene rearrangement, and DNA replication. Defective DSB repair is associated with developmental and immunological disorders and promotes carcinogenesis in humans (1). To avoid chromosomal alterations and rearrangements, cells must detect and repair DSBs timely and properly. Eukaryotes respond to DSBs by promptly initiating a multipronged DNA damage response, which involves the initiation of a cell cycle checkpoint and DNA repair. The cell cycle checkpoint is an intricate signal transduction pathway that involves DNA damage sensing, a slowing down or inhibition of cell cycle progression, and DNA repair (2).

The yeast *Saccharomyces cerevisiae* Tel1 and Mec1 protein kinases are orthologs of mammalian ataxia telangiectasia-mutated (ATM) and ATM- and Rad3-related (ATR), respectively. They are essential regulators of cell cycle checkpoint initiation in yeast (3, 4). Tel1 and Mec1 belong to a superfamily of protein kinases that share a common C-terminal phosphatidylinositol-3′-OH kinase–like kinase (PIKK) domain. All members of the PIKK family are very large proteins (>250 kDa), in which the C-terminal catalytic kinase domain makes up only 5–10% of the total sequence. The nonkinase regions of PIKKs are comprised largely of tandem HEAT (Huntington, elongation factor 3, A subunit of protein phosphatase 2A, and TOR1) repeats and show very little sequence homology even within subfamilies. Structural analyses have revealed that HEAT repeats form helical structures that form large curved superstructures (5–7). In addition to harboring the kinase domain, the C-terminal region of PIKKs is also very highly conserved (8, 9). Recent structural studies of *Schizosaccharomyces pombe* Tel1 show two Tel1 molecules that interact through the kinase and C-terminal domain to form a dimer (Fig. 1*A*) (10).

Tel1 (ATM) and Mec1 (ATR) respond to different forms of DNA damage. Although Mec1 is activated by ssDNA coated with the single-stranded binding factor RPA, Tel1 responds primarily to DSBs (11–13). However, they share an overlapping number of downstream phosphorylation targets and show partial redundancy in their checkpoint function (4). One of the initial targets of Tel1 in *S. cerevisiae* is histone H2A. Phosphorylation of H2A marks the chromatin surrounding the DNA lesion and is important for recruitment and retention of DNA repair proteins (14). Phosphorylated H2A is bound by the scaffold adaptor protein Rad9. The association of Rad9 with chromatin facilitates recruitment of the effector kinase Rad53, the budding yeast functional homolog of mammalian Chk1 and Chk2 kinases (15). Phosphorylation of Rad53 by Tel1, followed by further autophosphorylation of Rad53, results in full activation of Rad53 (16). Rad53 has many downstream targets, some of which couple cell cycle arrest with damage repair (12, 16, 17).

Recruitment of Tel1 to sites of DNA damage depends on Xrs2 (human Nbs1) protein. Xrs2 is a subunit of the Mre11–

This work was supported in part by NIGMS, National Institutes of Health Grant GM118129 (to P. M. B.) and National Science Foundation Graduate Research Fellowship 2014157291 (to S. H.). The authors declare that they have no conflicts of interest with the contents of this article. The content is solely the responsibility of the authors and does not necessarily represent the official views of the National Institutes of Health.

This article contains Figs. S1–S3 and supporting text.

[1] Present address: Intellia Therapeutics, Cambridge, MA 02139.

[2] To whom correspondence should be addressed. Tel.: 314-362-3772; Fax: 314-362-7183; E-mail: burgers@wustl.edu.

[3] The abbreviations used are: DSB, double-stranded DNA break; ATM, ataxia telangiectasia–mutated; ATR, ATM- and Rad3-related; PIKK, PI3K-related protein kinase; HEAT, Huntington, elongation factor 3, A subunit of protein phosphatase 2A, and TOR1; ssDNA, single-stranded DNA; MRX, Mre11–Rad50–Xrs2; MRN, Mre11–Rad50–Nbs1; RPA, replication protein A.

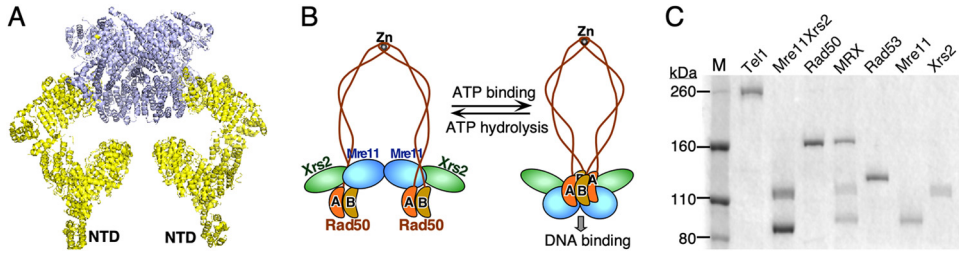

Figure 1. Tel1 kinase and the MRX complex. *A*, Tel1 and ATM kinases exist as dimers. The structure shown is that of human ATM (PDB code 4JSV). *Yellow*, HEAT repeats; *blue*, kinase and kinase-associated domains. *NTD*, N-terminal domain. *B*, schematic of the MRX complex in the presence and absence of ATP. The model is based on structural analysis of archaeal MR complexes. ATP binding by Rad50 transforms MRX from an open to closed conformation (see text for details). *C*, 7% SDS-PAGE analysis of purified Tel1, MRX, and MRX subunits and Rad53kd. Staining was performed with Coomassie Blue. *M*, size markers.

Rad50–Xrs2 (MRX) complex (18, 19). The MRX (human MRN) complex is involved in recognition and processing of DSBs. Mre11 and Rad50 are highly conserved and are found in all forms of life. Xrs2/Nbs1 is only present in eukaryotes and is not well conserved at the primary sequence level (20). MRX has several enzymatic and scaffolding properties and plays major roles in DNA break metabolism. It is a crucial player in all aspects of DSB processing: damage detection, cell cycle checkpoint initiation, and facilitating and catalyzing repair of the lesion (2, 21, 22). Mre11 belongs to the λ phosphatase family of enzymes and has both endo- and exonuclease activities (23, 24). Studies of budding yeast Mre11 show that mutations ablating its nuclease activity cause severe meiotic defects but result in only mild IR sensitivity, suggesting that the Mre11 nuclease activity is largely dispensable for DSB repair (25, 26). Rad50 belongs to the ABC transporter family of ATPases and shares structural features with structural maintenance of chromosome proteins (20, 27, 28). Its ATP-binding domains are split and located at the N- and C termini, separated by long coil-coiled domains (29, 30) (Fig. 1*B*). Active ATPase sites are only formed when two Rad50 molecules dimerize in an ATP-dependent manner (27). A conserved zinc hook at the apex of the coil-coiled region, distal from the ATPase domains, also mediates Rad50 dimerization (31). The ATPase domains of Rad50, along with the nuclease and DNA binding regions of Mre11, make up the catalytic core of the MRX complex (32, 33). Upon ATP binding by Rad50, this catalytic core retains a closed conformation, whereas ATP hydrolysis releases the MRX complex from the DNA (27, 34–37) (Fig. 1*B*).

Critical studies of the mammalian ATM and the MRN complex have resulted in a mechanistic framework for checkpoint initiation to DSBs (38). In an independent approach, extensive genetic studies of *S. cerevisiae* Tel1 and the MRX complex have given us a comprehensive understanding of where and how these factors function in various DNA metabolic pathways and which activities and/or domains are essential in each of these pathways (2, 21). However, until now, biochemical studies with purified yeast proteins have been lacking. In this study, we present biochemical data that illuminate how DNA and MRX orchestrate the activation of the Tel1 checkpoint kinase. We show that dsDNA is indispensable for stimulation of Tel1 kinase by MRX. A DNA length with a minimum of 80 bp is required for robust activation. Furthermore, DNA wrapped up into a nucleosome is ineffective. Surprisingly, dsDNA ends were not required for activation of Tel1 by MRX *in vitro*, even though, on small DNA effectors, a significant stimulatory function of DNA ends can be detected. Analysis of individual subunits and different heterodimeric pairs of MRX in the presence of DNA reveal that Rad50 is critical for activating Tel1. This stimulatory effect of Rad50 is absolutely dependent on its ATPase activity.

Results

DNA is required for MRX to fully stimulate Tel1

Previously, we described the overproduction and purification of *S. cerevisiae* Tel1 from yeast and described an initial structural analysis (6). When Tel1 was examined by EM, the main species was that of a dimer. Cryo-EM studies of human ATM and *S. pombe* Tel1 show that these orthologs are also homodimeric in structure (10, 39).

To allow for a comprehensive biochemical analysis of the MRX complex in its stimulation of Tel1 kinase activity, we purified each subunit separately from yeast, as well as the heterodimeric Mre11–Xrs2 complex. However, these highly purified preparations, particularly the Mre11–Xrs2 preparation, consistently showed protein kinase activity in the absence of Tel1 addition. In part, the contaminating kinase activity could be assigned to Tel1 itself, which copurified with these subunits. Because each subunit of the MRX complex interacts with Tel1 (see below), this finding was not unexpected. However, even when the MRX subunits were purified from a *tel1*Δ strain, detectable kinase activity remained. Mass spectrometry analysis of the purified preparations identified Tda1 as the co-purifying kinase (data not shown). *TDA1* shows genetic interactions with topoisomerase 1, suggesting that it may play a role in DNA metabolism (40). A potential role of Tda1 in MRX-dependent DNA metabolic processes remains to be investigated. When we purified the MRX subunits and subassemblies from a *tel1*Δ *tda1*Δ strain of yeast, essentially no contaminating protein kinase activity was observed (Fig. 2*A*, *lane 2*), and these preparations were used in all of our studies (Fig. 1*C*).

To study the protein kinase activity of Tel1, we used the downstream effector kinase Rad53, which is a physiological Tel1 substrate (12). The catalytically inactive form Rad53kd was used so that all observable protein phosphorylation was Tel1-dependent. In addition, the general PIKK substrate PHAS-I was used in several experiments (41), to query whether MRX stimulation of Tel1 kinase activity was specific for Rad53 as a substrate or a more general property.

Fig. 1*A* summarizes the critical aspects of the assay, which show that Tel1 kinase activity is weakly stimulated by either

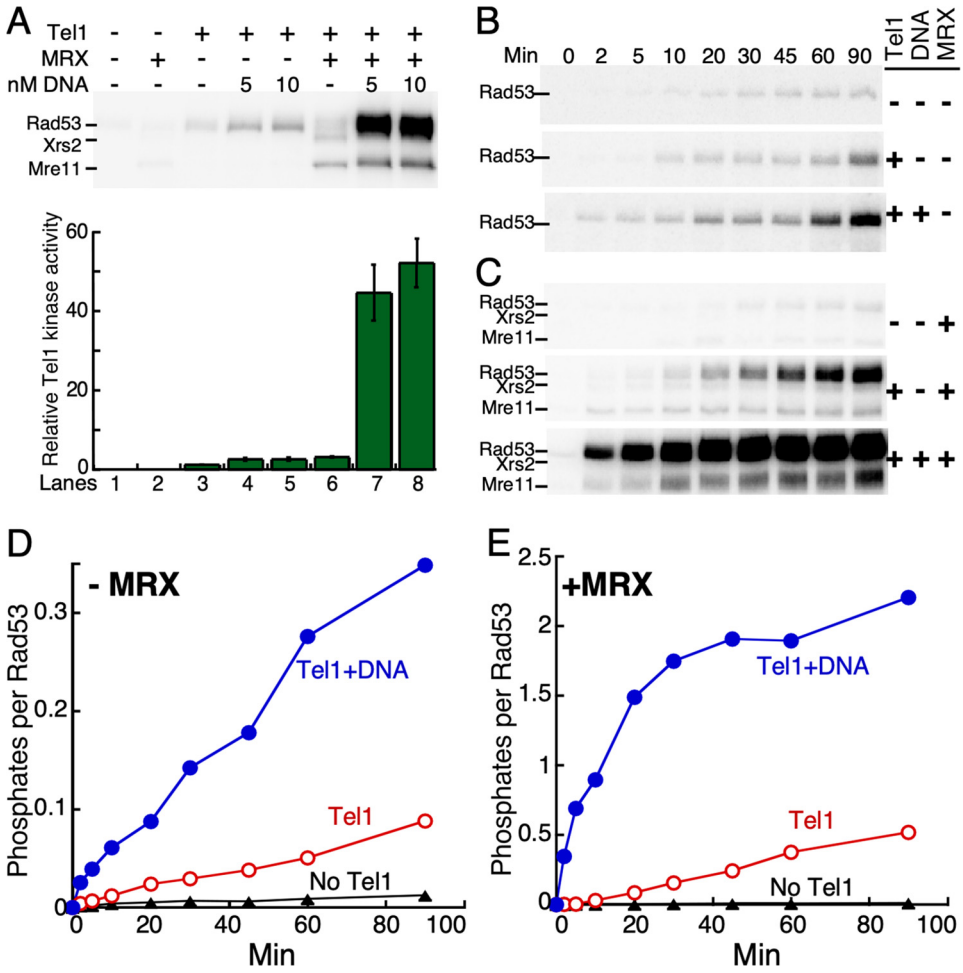

Figure 2. MRX and DNA synergistically activate Tel1 kinase. *A*, standard kinase reactions contained 200 nM Rad53kd and 50 μM [γ-^{32}P]ATP in kinase buffer with or without 30 nM MRX and the indicated concentration of 2-kb linear DNA. Kinase reactions were initiated with 5 nM Tel1 (*lanes 1* and *2* are negative controls). Reactions were stopped after 15 min at 30 °C and analyzed by 7% SDS-PAGE, followed by phosphorimaging. *Top panel*, a representative experiment. *Bottom panel*, phosphorylation of Rad53 was quantified and plotted as -fold increase of Tel1 kinase activity with *lane 3* set at 1. Averages and standard errors were derived from three independent experiments. *B* and *C*, time course analyses of Rad53 phosphorylation under standard conditions with 5 nM Tel1, 5 nM linear 2-kb DNA, and 30 nM MRX where indicated. *D*, quantification of the data in *B*. *E*, quantification of the data in *C*. Note the different *y* axis scales in *D* and *E*. A representative of two independent experiments is shown. In *A*–C, the migration of GST-Rad53kd (118 kDa), Xrs2 (96 kDa), and Mre11 (77 kDa) is as shown.

DNA or MRX alone, but both DNA and MRX show strong synergism. This assay was followed by comprehensive time course analyses of each of the conditions. The weak activity of Tel1 alone (0.065 phosphates transferred to Rad53 per minute per Tel1 monomer) was stimulated about 2- to 3-fold in the presence of linear 2-kb plasmid DNA (Fig. 2, *B* and *D*). Without DNA, the MRX complex also increased Tel1's basal activity 2- to 3-fold (Fig. 2, *C* and *E*). The presence of both DNA and MRX in the reaction resulted in a synergistic, 20- to 30-fold increase in Rad53 phosphorylation (Fig. 2, *C* and *E*). The synergistic stimulation of Tel1 by MRX and DNA is not specific to Rad53 as a substrate; it was also observed with PHAS-I, a commonly used substrate to probe the ATM/ATR family of kinases (Fig. S1*A*). In these assays, we had preassembled the MRX complex at 0 °C for 1 h prior to addition to the assay. To assess whether MRX preassembly is required, we either mixed the individually purified subunits of MRX at 0 °C for 1 h and added the pre-assembled complex to the assay or added them to the assay individually. In both cases, saturation was achieved at 10–20 nM MRX with 5 nM Tel1, indicating that preassembly was not required (Fig. S1, *B* and *C*). Therefore, we routinely used 30 nM MRX unless indicated otherwise.

A titration of the kinase substrate PHAS-I in the Tel1 assay in the presence of MRX, either with or without DNA present, gave an approximately linear dose–response curve up to 20 μM PHAS-I, indicative of a weak association of this substrate with Tel1 (Fig. S1*D*). Given these results, we cannot conclude whether DNA enhances the affinity of kinase substrates for MRX·Tel1, which would be a possible explanation for the observed synergism. Finally, Tel1 also phosphorylates the Xrs2 and Mre11 subunits of MRX (Fig. 2*A*), as it does in the cell in response to DNA damage (18, 42).

Nucleosome-free dsDNA is the preferred effector for Tel1/MRX

The homologous recombination repair pathway involves resection of double-stranded breaks by 5′-3′ exonucleases to generate ssDNA 3′ ends that are coated by the single-stranded DNA binding protein RPA (43). As resection proceeds and the 3′ overhangs increase in length, Tel1 activity is attenuated, and the checkpoint response is switched to that of a Mec1-mediated

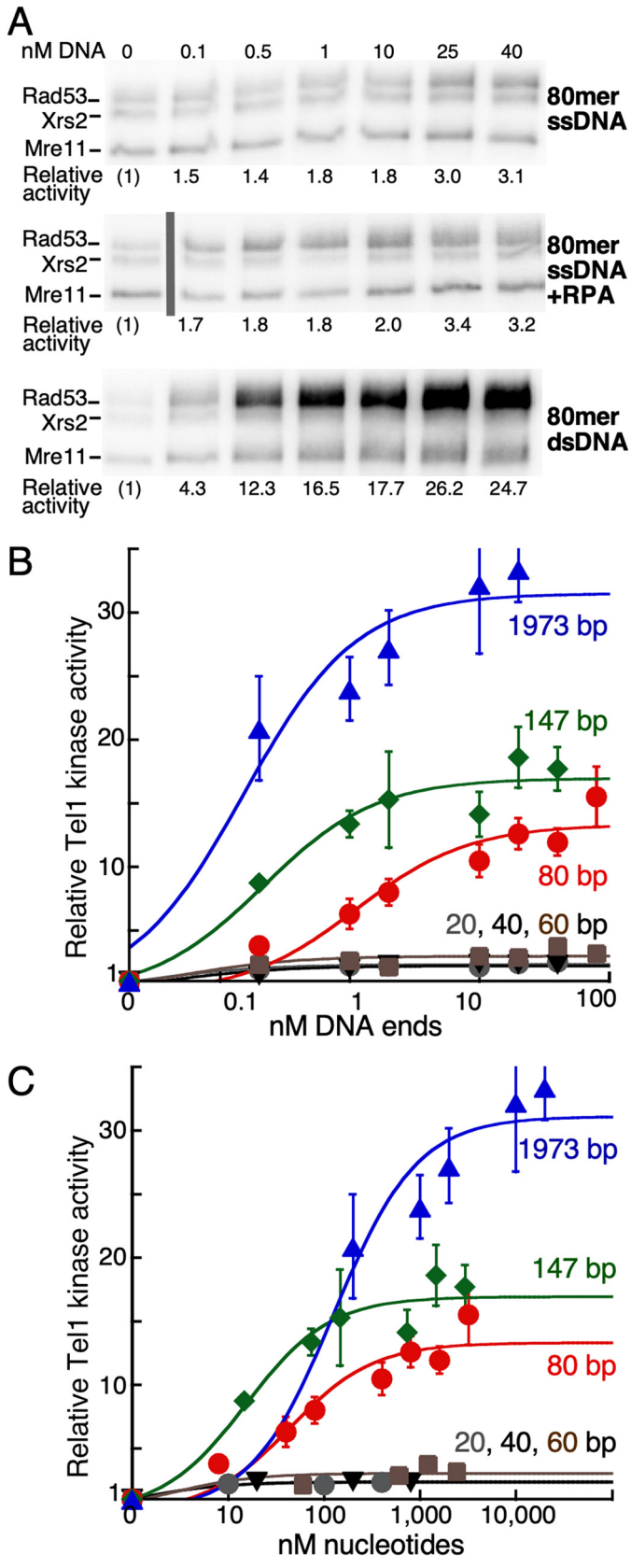

Figure 3. MRX·Tel1 exhibits a preference for long dsDNA. *A*, standard kinase reactions contained 5 nM Tel1, 30 nM MRX, 200 nM Rad53, and the indicated concentrations of 80-mer ssDNA with or without RPA or 80-mer dsDNA. The amount of RPA required to coat ssDNA was calculated for each DNA concentration with a single RPA trimer coating 30 nt. Relative Tel1 activity was calculated by setting the reaction without DNA to 1 (*lane 1*). The first lane in the ssDNA/RPA experiment comes from a different gel in the same experiment. The *gray bar* indicates the discontinuity. The migration of GST-Rad53kd (118 kDa), Xrs2 (96 kDa), and Mre11 (77 kDa) is as shown. *B*, standard kinase reactions contained 5 nM Tel1, 30 nM MRX, 200 nM Rad53, and increasing concentrations of linear dsDNA molecules with the indicated lengths. Data were plotted as a function of DNA end concentrations in a log plot. Relative Tel1 kinase activity was calculated by setting the reaction without DNA to 1. Averages and standard errors were derived from four independent experiments. *C*, the same data were plotted as a function of total DNA as nucleotide concentrations.

response (26). Previous studies with human ATM and MRN showed that kilobase-long dsDNA substrates were required to detect stimulation of ATM kinase activity (44). Here the sensitivity of our *in vitro* kinase assay enabled us to evaluate the roles of DNA strandedness, structure, and length as effectors for Tel1. A single-stranded 80-mer oligonucleotide was inactive for stimulation, whether coated with RPA or not, whereas the double-stranded form showed significant activity (Fig. 3*A*). This is in direct contrast to Mec1, which shows optimal activity on RPA-coated ssDNA (45). These findings are consistent with the proposed model where stretches of RPA-coated ssDNA resulting from DNA end resection mediate the transition from a Tel1- to a Mec1-dependent checkpoint response (46).

We next probed the DNA length requirement for stimulation. We compared double-stranded oligonucleotides in a size range of 20–80 bp, 147 bp, and a 2-kb linear plasmid DNA (Fig. 3, *B* and *C*). This analysis showed that, up to a length of 60 bp, there was little to no stimulation. The 147-mer dsDNA showed substantially higher activity than the 80-mer. A further increase in the effector DNA length to 2 kb showed another 2-fold increase in maximal activity. The activity data were plotted as a function of the concentration of dsDNA ends (Fig. 3*B*). Unexpectedly, the 2-kb linear DNA showed half-maximal activation at merely 0.1 nM DNA ends. If only DNA ends would be active in the MRX·Tel1 assay, given that the assay contains 2.5 nM Tel1 dimers, then half-maximal activation should occur at an end concentration of 1.25 nM DNA ends or more, depending on the affinity of MRX·Tel1 for ends. This titration experiment alone suggests that internal sites must be active for optimal stimulation of Tel1. The 147-mer dsDNA gave half-maximal activation at 0.2 nM ends and the 80-mer at 1.1 nM ends (Fig. 3*B*). Therefore, only the half-maximal concentration of the 80-mer is consistent with the model that only DNA ends serve as effectors of MRX·Tel1.

The data were replotted as a function of the total nucleotide concentration (Fig. 3*C*). Half-maximal stimulation was reached at 45 nM, 16 nM, and 125 nM nucleotide concentration for the 80-mer, 147-mer, and 2-kb DNA, respectively. Although the total data indicate that some variation in the strength of DNA effectors may occur, possibly because of sequence and/or DNA composition contexts, they also indicate that internal sites serve as effectors of MRX·Tel1. Consequently, the large number of potential internal binding sites on the 2-kb DNA contribute substantially to stimulation.

One possible model for Tel1 activity that maintains a requirement for DNA ends is one in which DNA ends are required for loading of MRX·Tel1 but that subsequently the complex can slide to internal regions along the dsDNA. This would allow assembly of additional complexes that are all active

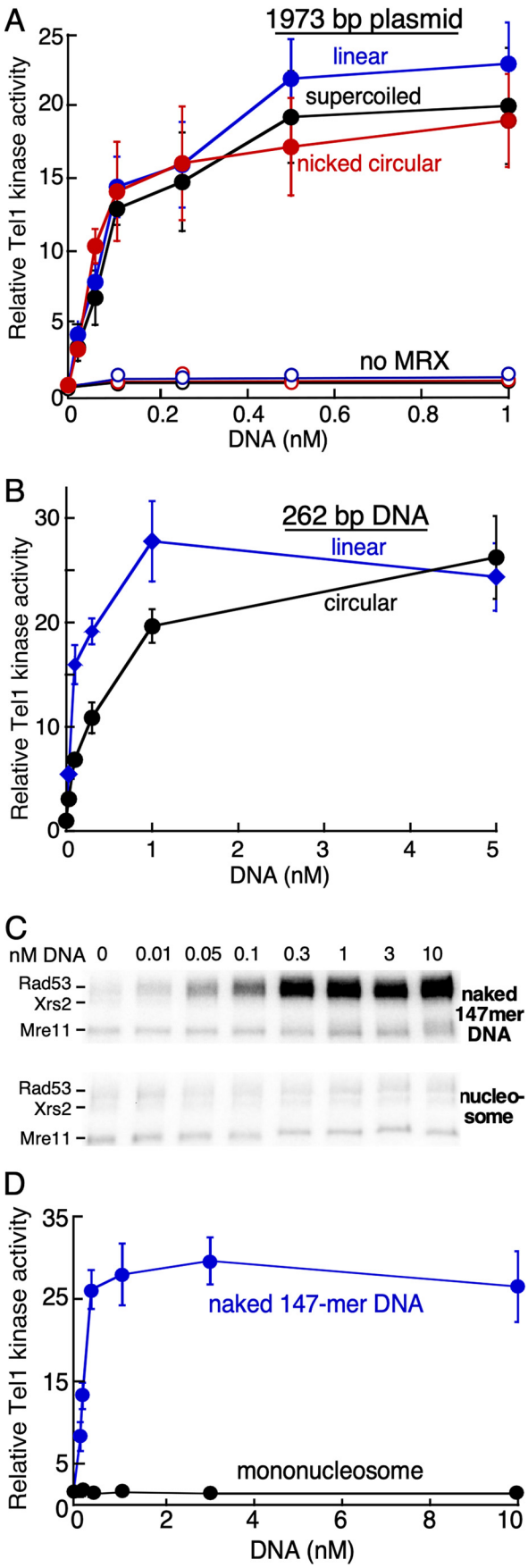

Figure 4. Requirement for nucleosome-free DNA but not DNA ends for Tel1 activation. *A*, kinase reactions contained 5 nM Tel1, 30 nM MRX, 200 nM Rad53, and increasing concentrations of 2 kb DNA with the indicated structures. Relative Tel1 kinase activity was calculated by setting the reaction without DNA to 1. Averages and standard errors were derived from five independent experiments. The "no MRX" control titrations are shown for each DNA substrate. *B*, kinase reactions contained 5 nM Tel1, 30 nM MRX, 200 nM Rad53, and increasing concentrations of either linear or circular 262-bp DNA. Relative Tel1 kinase activity was calculated by setting the reaction without DNA to 1. Averages and standard errors were derived from three independent experiments. *C*, standard kinase reactions contained 5 nM Tel1, 30 nM MRX, 200 nM Rad53, and increasing concentrations of either 147-bp naked DNA or the nucleosome assembled on the same DNA. A representative experiment is shown. The migration of GST-Rad53kd (118 kDa), Xrs2 (96 kDa), and Mre11 (77 kDa) is as shown. *D*, quantification of four independent experiments with standard errors shown.

for kinase activity. This model would explain why the half-maximal concentration of the 2-kb effector is over 10 times lower than the concentration of MRX·Tel1 complexes. To test this model, we carried out an assay with the 2-kb plasmid either in the supercoiled, nicked, or linear form (Fig. 4*A*). In control experiments, we showed that the supercoiled and the nicked DNA effectors remained intact during the assay (data not shown). Mre11 is a known nuclease; however, Mre11 nuclease activity requires manganese, whereas our studies were carried out in magnesium-containing buffers (47, 48).

Although the stimulation of Tel1 activity by MRX on linear DNA was slightly higher than on supercoiled or nicked DNA, the difference was of low statistical significance. Therefore, DNA ends are not essential for MRX-dependent Tel1 kinase activity. However, are ends stimulatory? The result shown in Fig. 4*A* would be expected if the contribution by the vast excess of internal sites masked the stimulatory contribution stemming from DNA ends. To reveal a possible contribution by DNA ends, we repeated this experiment with a much shorter DNA, 262 nt in length (Fig. S2*A*). Indeed, with this small DNA, the linear form is more active than the circular form, even though the circular DNA shows robust activity at higher DNA concentrations (Fig. 4*B*). Collectively, these data indicate the significance of internal DNA binding sites for MRX-dependent activation of Tel1. In support of the internal entry model, proficient internal loading of MRX has been shown in single-molecule studies (49).

So far, our experiments were carried out with naked DNA. We next determined whether nucleosomal DNA showed activity in our assay, but it did not. First, assembly of the DNA into a nucleosome caused inhibition of the MRX-independent but DNA-dependent activation of Tel1's basal kinase activity (Fig. 2*A* and Fig. S2*B*). With the complete system, we observed at least a 100-fold difference in the ability of the naked 147-mer to activate Tel1 compared with the same DNA wrapped up into a nucleosome (Fig. 4, *C* and *D*). The inhibitory effect of mononucleosomal DNA was recapitulated when PHAS-I was used instead of Rad53 as a substrate for Tel1 (Fig. S2*C*). We carried out two additional control experiments. We showed that histone octamers themselves, *i.e.* not bound up in a nucleosome, did not cause inhibition of Tel1 (Fig. S2*D*). Furthermore, we showed that the binding of DNA by general dsDNA binding proteins, such as HMGB-1, is also inhibitory, albeit less absolutely than that by the nucleosome (Fig. S2*E*).

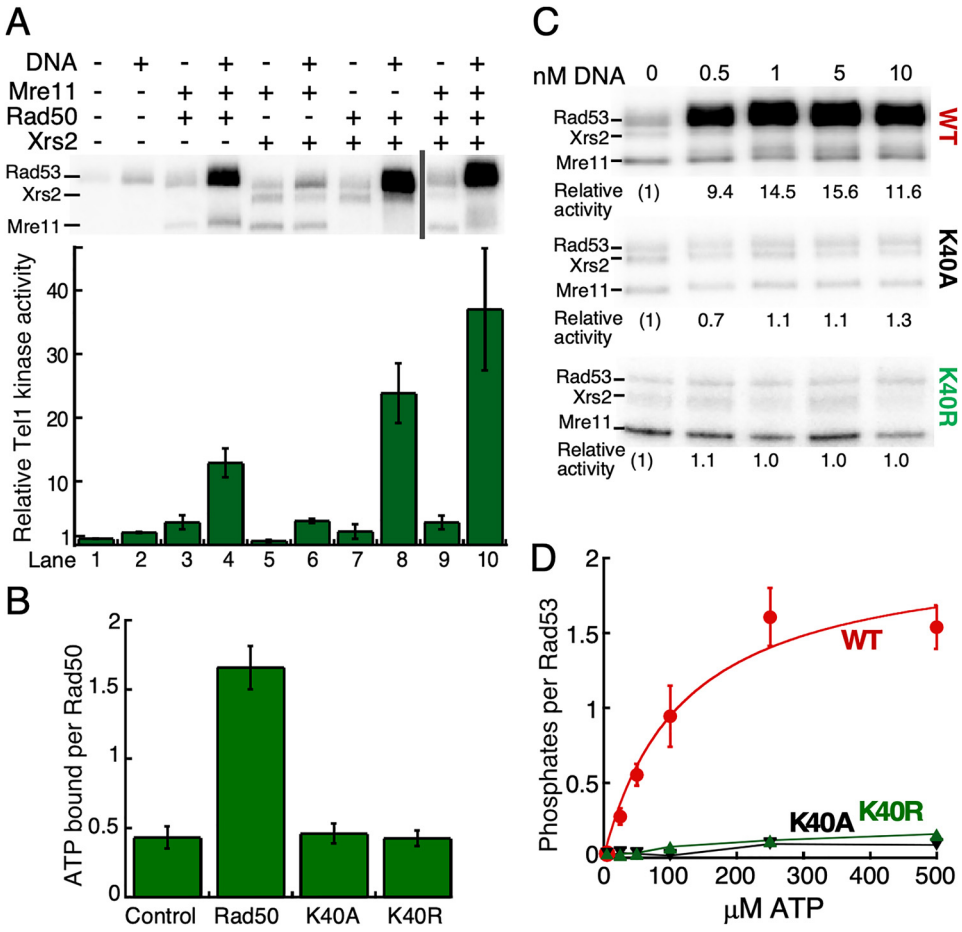

Figure 5. Rad50 ATP binding is required for Tel1 activation. *A*, standard kinase reaction with 5 nM Tel1, 200 nM Rad53, and 30 nM MR, MX, RX, or MRX with or without 5 nM linear 2-kb DNA. *Top panel*, representative of three independent experiments. The *right two lanes* were derived from a different gel in the same experiment (both gels are shown in Fig. S3*A*). The *gray bar* indicates the discontinuity. *Bottom panel*, quantification and standard errors. Relative Tel1 kinase activity was calculated by setting Tel1 alone (*lane 1*) to 1. *B*, nitrocellulose filter binding assays of the binding of 50 μM [γ-^{32}P]ATP to 500 nM WT or mutant MRX. *Control*, no MRX (see details under "Experimental procedures"). Quantification of four independent experiments with standard errors is shown. *C*, kinase assays were carried out using 5 nM Tel1; 200 nM Rad53; 30 nM MRX, MR(K40A)X, or MR(K40R)X; and increasing concentrations of 80-mer dsDNA. A representative of two experiments is shown. *D*, standard kinase reaction with 5 nM Tel1; 200 nM Rad53; 30 nM MRX, MR(K40A)X, or MR(K40R)X; 5 nM linear 2-kb DNA; and increasing concentrations of [γ-^{32}P]ATP. Quantification of three independent experiments with standard errors is shown. In *A* and C, the migration of GST-Rad53kd (118 kDa), Xrs2 (96 kDa), and Mre11 (77 kDa) is as shown.

Rad50, but not Xrs2 or Mre11, is essential for DNA-dependent activation of Tel1 by MRX

To determine which of the subunit(s) of the MRX complex are essential for Tel1 kinase activation, we measured Tel1 stimulation by each of the subunits alone and by the different heterodimeric complexes. These experiments were carried out in the presence of saturating concentrations of the 2-kb linear DNA effector. None of the single subunits alone stimulated Tel1 kinase (Fig. S3*A*), suggesting that the mere physical association of these factors with Tel1 (see below) is insufficient for activation. The Mre11–Xrs2 pair was also unable to stimulate kinase activity (Fig. 5*A*, *lane 6*). In contrast, both the Rad50–Mre11 and Rad50–Xrs2 pairs showed substantial kinase activation (Fig. 5*A*, *lanes 8* and *10*). These data indicate that although neither Mre11 or Xrs2 is required, the interaction of either subunit with Rad50 is a prerequisite for Rad50 to function in Tel1 activation. The activity of the complete MRX complex was 1.5-fold higher than that of the Rad50–Xrs2 pair. Two sets of observations exclude the possibility that the activity of the heterodimers is caused by cross-contamination of the Rad50–Mre11 assay with Xrs2 or the Rad50–Xrs2 subunit with Mre11. First, the Rad50–Mre11 assay lacks detectable phosphorylated Xrs2, and the Rad50–Xrs2 assay lacks detectable phosphorylated Mre11 (Fig. 5*A*, *lanes 4* and *8*, respectively). Second, the same robust activity of the Rad50–Xrs2 pair was observed when Rad50 was purified from a yeast *mre11*Δ mutant and Xrs2 from *Escherichia coli*, eliminating the possibility of contamination with Mre11 (Fig. S3*B*).

Rad50 belongs to the ABC transporter family of ATPases and shares structural similarities to structural maintenance of chromosome proteins (38). The ATP-dependent activities of *S. cerevisiae* Rad50 are required for all of its functions in DNA repair, as ATPase-dead mutants show a similar phenotype as *rad50*Δ mutants. DNA stimulates the ATPase activity of Rad50 alone or of the MRX complex, and at least one study shows that ends are important for this stimulation (50). We also observed that the linear plasmid was significantly more stimulatory for the ATPase than the circular plasmid DNA (Fig. S2*F*). As discussed below, ATP turnover is not important for MRX-dependent activation of Tel1 but ATP binding is. To test the ATP-

binding requirement, we mutated the conserved Walker A-box lysine residue to either alanine or arginine, which has been shown to inactivate its ATPase activity (51). Neither mutant MRX complex showed detectable ATP binding (Fig. 5*B*). Furthermore, the mutant complexes were inactive for Tel1 stimulation (Fig. 5*C*). We further tested whether the Rad50–K40A and Rad50–K40R mutant MRX complexes retained partial activity in stimulating Tel1 at higher concentrations of ATP. However, even at ATP concentrations as high as 0.5 mM, no significant stimulation by the mutant complexes was observed (Fig. 5*D*). Thus, the ATP-dependent activity of Rad50 is essential for the stimulatory role of MRX.

Each member of MRX interacts individually with Tel1

To further increase the knowledge of the system, we probed the physical interactions between each of the MRX subunits with Tel1. The C-terminal region of Xrs2 has been shown to physically associate with Tel1, and this association is required for localizing Tel1 to DSBs (18, 19). To determine whether Mre11 and Rad50 also interact with Tel1, we performed a pull-down experiment with the individual subunits (Fig. 6*A*). GST-Tel1, or GST as a control, was incubated with each subunit together with GSH beads. The beads were washed three times with buffer to remove nonspecifically bound proteins and subjected to SDS-PAGE analysis. Proteins were visualized using silver staining (Fig. 6*A*). Tel1 was able to pull down each individual subunit, indicating that each subunit binds Tel1. Mre11 showed the most robust interaction with Tel1. As the Tel1-Rad50 interaction appeared rather weak, we repeated the pull-down experiment using a more sensitive Western blot analysis with anti-Rad50 antibodies (Fig. 6*B*, *lane 5*). This experiment positively established the interaction between Rad50 and Tel1. In addition, we probed Rad50 interactions with Mre11 and Xrs2 (Fig. 6*B*, *lanes 3* and *4*, respectively). As a positive control, we confirmed the known interaction of Rad50 with Mre11 (24). A previous study established interactions between human Rad50 and Nbs1 (52). Our data extend this interaction network to yeast Rad50 with Xrs2 (*lane 4*). These experiments establish that each of the subunits of MRX interact with each other and with Tel1.

Discussion

Prior to this biochemical analysis of the yeast MRX·Tel1 checkpoint complex, only the mammalian MRN·ATM complex had been studied in a purified protein system, in a series of insightful studies by Paull (53). Although a comparison of the yeast and mammalian systems shows some broad similarities, it also reveals critical differences that may have a decisive effect on the mechanism of action by these checkpoint complexes in the different organisms. Human ATM kinase activity is stimulated about 100-fold when both MRN and kilobase-long DNA are present, and there is an absolute requirement for dsDNA ends (44). There is also a requirement for Mn^{2+} rather than Mg^{2+}; however, the nuclease activities of Mre11, which also depend on Mn^{2+}, are dispensable for kinase activation (54). ATM dimer-to-monomer transitions are mediated by phosphorylation and acetylation of specific residues (55, 56). Based on mutational studies of ATM sites that are subject to post-

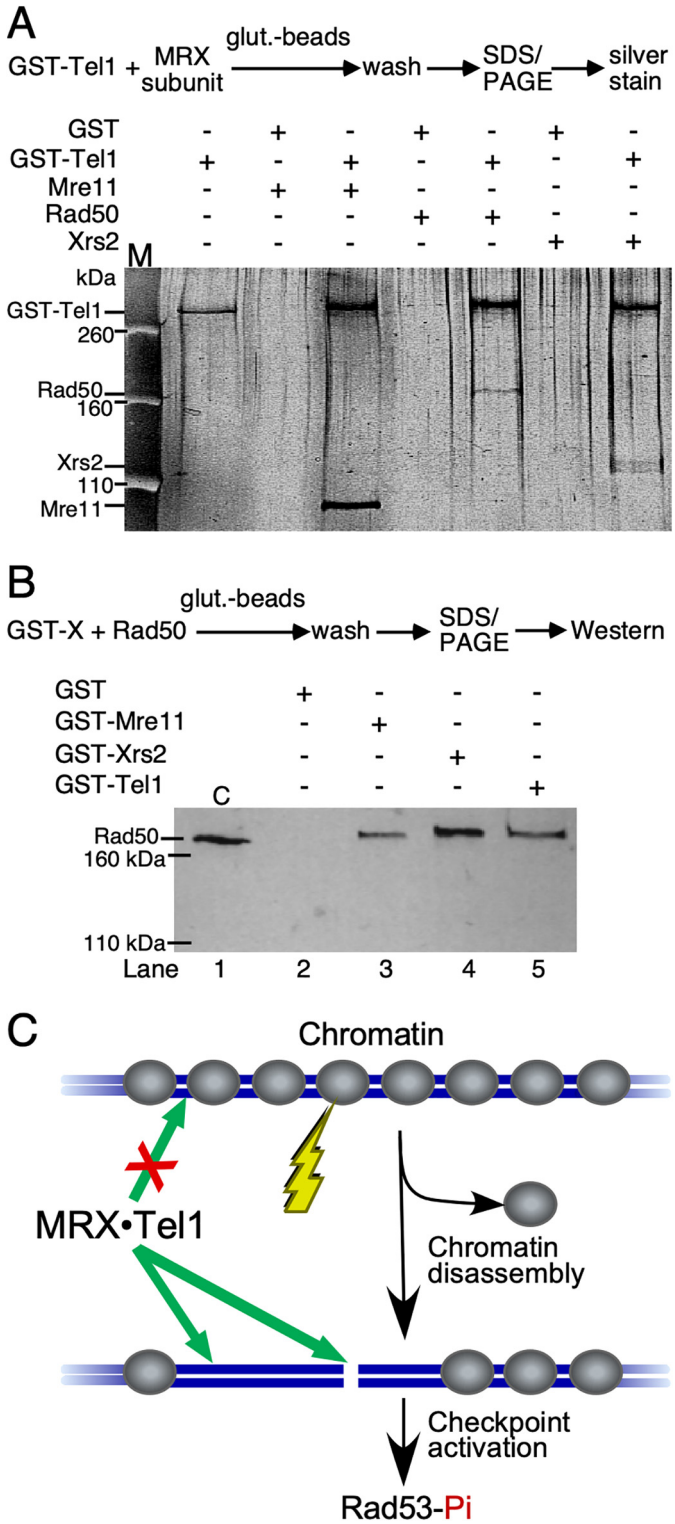

Figure 6. MRX·Tel1 interaction network. *A*, purified MRX subunits were incubated with GST-tagged Tel1 in the presence of glutathione-Sepharose beads (*glut.-beads*). The beads were washed, and bound proteins were analyzed by 7% SDS-PAGE, followed by silver staining ("Experimental procedures"). GST was used as a negative control for each subunit, as indicated. A representative of three independent experiments is shown. *M*, size markers. *B*, purified Rad50 subunit was incubated with either GST-tagged Mre11, Xrs2, or Tel1. Bound Rad50 was analyzed by Western blotting with anti-Rad50 antibody. *Lane 2*, negative control; binding of Rad50 to GST. *C*, model for MRX·Tel1 recruitment to non-nucleosomal DNA (see text for details).

translational modification, it has been proposed that the active form of ATM is that of a monomer (44, 55). However, the orthologous mouse ATM mutants are without an *ataxia telangiectasia* phenotype, suggesting that regulation of ATM activity in human and mouse may not be conserved (57). Importantly, the assembly state of active ATM or Tel1 when bound to DNA still remains to be established.

Our biochemical analysis was carried out under near-physiological conditions with Mg^{2+} as cofactor. The 50- to 100-fold stimulation of Tel1 kinase activity when both MRX and DNA are present allowed us to attach statistical significance to the observation that either MRX or DNA alone stimulates the kinase activity 2- to 3-fold (Fig. 2, *D* and *E*). Our study was aided by rigorous elimination of contaminating and cross-contaminating activities through isolation of the checkpoint proteins from appropriate yeast deletion strains (see "Results"). The dsDNA length requirement for activation was shorter for the yeast system, with nearly full activity achieved with a 147-mer DNA, whereas robust ATM activation required much longer DNA, 0.7 kb for partial activity and 2 kb for full activity (44). The fundamental difference between the human and the yeast system, however, is that MRX·Tel1 does not require DNA ends for maximal activity (Fig. 4*A*), whereas human MRN·ATM is absolutely dependent on DNA ends. The stimulation by DNA ends can only be observed on small DNA (Fig. 4*B*).

In principle, this surprising result is not incompatible with the known dsDNA break checkpoint activity of MRX·Tel1. Kinase activation is completely inhibited on nucleosomal DNA (Fig. 4, *C* and *D*). This result predicts that spontaneous activation of Tel1 kinase would not occur on undamaged, fully chromatinized chromosomes. However, extensive nucleosome disassembly has been documented at dsDNA breaks in yeast and in other organisms (58, 59). The resulting naked DNA is more than 0.5 kb in length in yeast, which is sufficient for robust MRX·Tel1 loading. This model of Tel1 activation at dsDNA breaks through its exclusion from normal chromatin is shown in Fig. 6*C*. The model does not exclude the possibility of other accessory factors further enhancing binding at dsDNA ends, but in our biochemical assay, there is no prerequisite for such factors.

Structural and biochemical studies based on archaeal and bacterial Mre11–Rad50 complexes (60), as well as biochemical and genetic studies of eukaryotic MRX(N) complexes have led to a model where ATP binding by Rad50 promotes DNA binding and Tel1 kinase activation (50, 61). ATP hydrolysis, on the other hand, releases the complex from DNA (Fig. 1*A*). Consistent with this model, Rad50 ATP-binding mutants show no activation of Tel1 activity (Fig. 5*C*). As expected, our analysis of the individual subunits of MRX showed that Rad50 is essential for Tel1 activation in the presence of dsDNA (Fig. 5*A*). But it is not sufficient, and either Mre11 or Xrs2 is also required. Possibly, because Rad50 alone shows very weak interactions with Tel1 (Fig. 6*A*), the additional interactions mediated by either Mre11 or Xrs2 strengthen complex formation with Tel1, leading to robust kinase activation. In yeast, all three subunits of MRX are essential for Tel1-dependent phosphorylation of Rad53 in response to zeocin, a dsDNA break–inducing agent, although Xrs2 is dispensable for several other functions of MRX, provided nuclear localization of Mre11–Rad50 is ensured (62).

When comparing the activation mechanism of $Tel1^{ATM}$ with that of the related PIKKs $Mec1^{ATR}$ and DNA-PK, it is interesting to note that Mec1 can be activated by an activator protein alone, such as $Dpb11^{TopBP1}$, or even by a peptide derived from an activator protein (63), whereas DNA-PK activation can be accomplished by DNA binding alone (64). In contrast, Tel1 requires both DNA and MRX, with Rad50 also requiring proficient ATP-binding capacity. A comprehensive description of the Tel1 activation mechanism will have to take into consideration that DNA and MRX individually stimulate Tel1 kinase activity 2- to 3-fold, but that both factors together show a profound synergism. Our studies show that Tel1 alone binds DNA proficiently and saturably in the absence of MRX (Fig. 2*D*), and Tel1 binds MRX proficiently in the absence of DNA (Fig. 6, *A* and *B*). Therefore, increases in binding affinities are unlikely explanations for the observed hyperactivity by the ternary complex. It is probable that DNA-induced conformational changes within the MRX complex are the driving force for Tel1 kinase activation. Whether kinase activation is a consequence of MRX- and DNA-mediated monomerization of Tel1 or whether other MRX- and DNA-induced conformational rearrangements of Tel1 result in its activation is currently not known and an important question for further investigation.

Experimental procedures

Yeast strains, DNA, and proteins

The strains used were BJ2168 (*MAT***a** *leu2–3,112 pep4–3 prb1–1122 prc1–407 trp1–289 ura3–52*), PY265 (*MAT***a** *can1 his3 leu2 trp1 ura3 pep4*Δ*::HIS3 nam7*Δ*::KanMX4*), PY335 (*MAT***a** *his3 leu2 trp1 ura3 pep4*Δ*::HIS3 tel1*Δ*::KanMX4 tda1*Δ*::NAT1*), and BY4741-Mre11 (*MAT***a** *his3*Δ*1 leu2*Δ*0 met15*Δ*0 ura3*Δ*0 mre11*Δ*::KanMX4*). The oligonucleotides used are listed in the supporting text.

Tel1 was overexpressed in yeast strain PY265 from the galactose-inducible plasmid pBL602 and purified as described previously (6). The protein was purified containing an N-terminal GST domain fusion. The GST domain was retained for the protein interaction studies in Fig. 6*A* but was cleaved off followed by heparin-agarose purification, as described previously (6), for all other experiments. Rad50 was overexpressed in BJ2168 or BY4741–Mre11 from the galactose-inducible plasmid pPM321 and purified as described previously (65). Rad50 mutants were made in this plasmid and purified similarly.

Plasmid pBL535 (pRS424-GAL (2 μM origin, *TRP1*) ZZ-3C-*XRS2, MRE11*) has the IgG-binding StrepA-ZZ tag fused to the N terminus of Xrs2, separated by a Prescission protease cleavage site, and Mre11 divergently expressed from the galactose-inducible *GAL1–10* promoter. The IgG-tagged Mre11–Xrs2 dimer was overexpressed in yeast strain PY335 from pBL535. After growth and galactose induction, cells were harvested and resuspended in a half-volume of 3× Hep_{200} buffer (30 mM HEPES (pH 7.8), 10% glycerol, 200 mM NaCl, 150 mM ammonium sulfate, 2 mM DTT, 0.1% Tween 20, 1 mM EDTA, 0.5 mM EGTA, 5 μM pepstatin A, 5 μM leupeptin, and 1 mM $NaHSO_3$; the suffix refers to mM NaCl in the buffer) and frozen in liquid

nitrogen as popcorn as described previously (66). The frozen cells were lysed by blending in dry ice in, treated with polyamin P, and centrifuged, and the supernatant was treated with ammonium sulfate and centrifuged as described previously (66).The ammonium sulfate pellet was resuspended in HEP_0 buffer (as HEP_{200} buffer but without NaCl) and incubated with IgG-Sepharose beads (GE Healthcare, 1 ml/100 g of frozen popcorn cells) for 4 h at 4 °C. The beads were washed with 50 column volumes of HEP_{300} supplemented with 0.02% E10C12 detergent. The beads were rotated gently overnight at 4 °C with 1 ml of HEP_{300} supplemented with Prescission protease to cleave the ZZ tag. The Mre11–Xrs2 dimer was further purified over a 1-ml heparin-agarose column. The protein was loaded in HEP_{300} buffer, the column was washed with 50 ml HEP_{300}, and the protein was eluted with HEP_{700} buffer.

Plasmid pBL532 (pRS424-GAL (2 μM ori, *TRP1*) GST-3C-*MRE11*) has GST fusion at the N terminus of Mre11, separated by a Prescission protease cleavage site, placed under control of the galactose-inducible *GAL1–10* promoter. Expression of Mre11 in yeast strain PY335 and purification were exactly as described for Mre11–Xrs2. Xrs2 was overexpressed in *E. coli* BL21-DE3-Star (Invitrogen) from plasmid pBL533 (pGEX-6P1-GST-3C-Xrs2). Cells were grown and induced at 37 °C using standard procedures. The cells were harvested and resuspended in an equal volume of 2× HEP_{200} buffer (including 5 μM bestatin and 1 μM E64, both from Sigma-Aldrich), subjected to a freeze–thaw cycle, incubated with 0.2 mg/ml lysozyme for 30 min on ice, and lysed by sonication. Polyamin P (40 μl of a 10% solution per milliliter of lysate) was added, and the lysate was cleared at 27,000 × *g* for 20 min. Solid ammonium sulfate (0.3 g per milliliter of cleared lysate) was added with stirring, and after 30 min, the precipitate was collected at 27,000 × *g* for 30 min and resuspended in 10 ml (per liter of induction culture) of the same buffer. After binding for 4 h to 1 ml of GSH-Sepharose, the beads were washed with 50 ml of buffer, followed by elution with 30 mM reduced GSH in HEP_{200} (but at pH 8.1). The eluted Xrs2 was further purified over a 1-ml heparin agarose column as described above. The MRX complex was formed by incubating equimolar amounts of Rad50 and Mre11–Xrs2 or the individual subunits at 0 °C for 1 h.

Tel1 kinase assay

The 10-μl standard assay contained 25 mM HEPES-NaOH (pH 7.6), 80 mM NaCl, 7 mM Mg acetate, 100 μg/ml BSA, 1 mM DTT, 50 μM ATP, 0.05 μCi [γ-^{32}P]ATP, 200 nM GST-Rad53kd, 30 nM MRX, and 5 nM linear 2-kb DNA (pUC19-Δ2, a 1973-bp plasmid derived from pUC19 cut with BamHI). Reactions were started with 5 nM Tel1 (monomer concentration) at 30 °C for 15 min, stopped with 4 ml of 2.5× SDS-PAGE loading dye, boiled, and separated on 7% SDS-PAGE gels. The gels were dried and exposed to a phosphor screen (GE Healthcare). Variations are indicated in the figure legends. pUC19-Δ2 was nicked with the BbvC1 nickase (New England Biolabs) for the experiment shown in Fig. 4*A*. Quantification of the data was carried out using ImageQuant software. Data were analyzed and plotted using KaleidaGraph software, which was also used to model the data in Figs. 3, *B* and *C*, and 5*D* to the Michaelis–Menten equation

GST pulldown experiments and ATP-binding studies

Purified MRX subunits (500 ng) were incubated with GST-tagged Tel1 (2 μg) in the presence of 50 μl of GSH-Sepharose beads in a total volume of 200 μl of HEP_{200} buffer (without protease inhibitors). After 4 h of incubation at 4 °C with rotation, the beads were subjected to three 0.5-ml washes with HEP_{200} to remove nonspecifically bound proteins. The beads were loaded in a spin column, centrifuged briefly to remove residual buffer, suspended in 50 μl of SDS-PAGE loading buffer, boiled, and spun, and the supernatant was analyzed by 7% SDS-PAGE. Visualization was by silver staining. Alternatively, the proteins were transferred to a PVDF membrane and processed further for Western blot analysis with anti-scRad50 antibodies (Thermo Fisher) using standard procedures.

Nitrocellulose filter binding experiments were performed as described previously (67) using 500 nM MRX in kinase buffer and 50 μM [γ-^{32}P]ATP in a 20-μl assay. After incubation at 0 °C for 30 min, the mixture was passed through a nitrocellulose membrane with gentle suction and washed with 2 × 0.5 ml of buffer. The dried filters were subjected to Cerenkov scintillation counting.

Author contributions—S. H., S. K., and P. M. B. conceptualization; S. H., S. K., and P. M. B. data curation; S. H. and P. M. B. formal analysis; S. H. and P. M. B. investigation; S. H. and P. M. B. writing - original draft; S. H., S. K., and P. M. B. writing - review and editing; P. M. B. resources; P. M. B. supervision; P. M. B. funding acquisition; P. M. B. project administration.

Acknowledgments—We thank Bonita Yoder for strain construction, Carrie Stith for general support with all aspects of this work, and Roberto Galletto for the Xrs2 overexpression plasmid.

References

1. Lavin, M. F., and Shiloh, Y. (1997) The genetic defect in ataxia-telangiectasia. *Annu. Rev. Immunol.* **15,** 177–202 CrossRef Medline
2. Oh, J., and Symington, L. S. (2018) Role of the Mre11 complex in preserving genome integrity. *Genes* **9,** E589 Medline
3. Abraham, R. T. (2001) Cell cycle checkpoint signaling through the ATM and ATR kinases. *Genes Dev.* **15,** 2177–2196 CrossRef Medline
4. Mallory, J. C., and Petes, T. D. (2000) Protein kinase activity of Tel1p and Mec1p, two *Saccharomyces cerevisiae* proteins related to the human ATM protein kinase. *Proc. Natl. Acad. Sci. U.S.A.* **97,** 13749–13754 CrossRef Medline
5. Perry, J., and Kleckner, N. (2003) The ATRs, ATMs, and TORs are giant HEAT repeat proteins. *Cell* **112,** 151–155 CrossRef Medline
6. Sawicka, M., Wanrooij, P. H., Darbari, V. C., Tannous, E., Hailemariam, S., Bose, D., Makarova, A. V., Burgers, P. M., and Zhang, X. (2016) The dimeric architecture of checkpoint kinases Mec1ATR and Tel1ATM reveal a common structural organization. *J. Biol. Chem.* **291,** 13436–13447 CrossRef Medline
7. Shiloh, Y. (2003) ATM and related protein kinases: safeguarding genome integrity. *Nat. Rev. Cancer* **3,** 155–168 CrossRef Medline
8. Bosotti, R., Isacchi, A., and Sonnhammer, E. L. (2000) FAT: a novel domain in PIK-related kinases. *Trends Biochem. Sci.* **25,** 225–227 CrossRef Medline
9. Ogi, H., Goto, G. H., Ghosh, A., Zencir, S., Henry, E., and Sugimoto, K. (2015) Requirement of the FATC domain of protein kinase Tel1 for localization to DNA ends and target protein recognition. *Mol. Biol. Cell* **26,** 3480–3488 CrossRef Medline

10. Wang, X., Chu, H., Lv, M., Zhang, Z., Qiu, S., Liu, H., Shen, X., Wang, W., and Cai, G. (2016) Structure of the intact ATM/Tel1 kinase. *Nat. Commun.* **7,** 11655 CrossRef Medline
11. Sanchez, Y., Desany, B. A., Jones, W. J., Liu, Q., Wang, B., and Elledge, S. J. (1996) Regulation of RAD53 by the ATM-like kinases MEC1 and TEL1 in yeast cell cycle checkpoint pathways. *Science* **271,** 357–360 CrossRef Medline
12. Usui, T., Ogawa, H., and Petrini, J. H. (2001) A DNA damage response pathway controlled by Tel1 and the Mre11 complex. *Mol. Cell* **7,** 1255–1266 CrossRef Medline
13. Zou, L., and Elledge, S. J. (2003) Sensing DNA damage through ATRIP recognition of RPA-ssDNA complexes. *Science* **300,** 1542–1548 CrossRef Medline
14. Downs, J. A., Lowndes, N. F., and Jackson, S. P. (2000) A role for *Saccharomyces cerevisiae* histone H2A in DNA repair. *Nature* **408,** 1001–1004 CrossRef Medline
15. Hammet, A., Magill, C., Heierhorst, J., and Jackson, S. P. (2007) Rad9 BRCT domain interaction with phosphorylated H2AX regulates the G_1 checkpoint in budding yeast. *EMBO Rep.* **8,** 851–857 CrossRef Medline
16. Usui, T., Foster, S. S., and Petrini, J. H. (2009) Maintenance of the DNA damage checkpoint requires DNA damage-induced mediator protein oligomerization. *Mol. Cell* **33,** 147–159 CrossRef Medline
17. Lee, S. J., Schwartz, M. F., Duong, J. K., and Stern, D. F. (2003) Rad53 phosphorylation site clusters are important for Rad53 regulation and signaling. *Mol. Cell. Biol.* **23,** 6300–6314 CrossRef Medline
18. Nakada, D., Matsumoto, K., and Sugimoto, K. (2003) ATM-related Tel1 associates with double-strand breaks through an Xrs2-dependent mechanism. *Genes Dev.* **17,** 1957–1962 CrossRef Medline
19. You, Z., Chahwan, C., Bailis, J., Hunter, T., and Russell, P. (2005) ATM activation and its recruitment to damaged DNA require binding to the C terminus of Nbs1. *Mol. Cell. Biol.* **25,** 5363–5379 CrossRef Medline
20. Aravind, L., Walker, D. R., and Koonin, E. V. (1999) Conserved domains in DNA repair proteins and evolution of repair systems. *Nucleic Acids Res.* **27,** 1223–1242 CrossRef Medline
21. Adelman, C. A., and Petrini, J. H. (2009) Division of labor: DNA repair and the cell cycle specific functions of the Mre11 complex. *Cell Cycle* **8,** 1510–1514 CrossRef Medline
22. Lamarche, B. J., Orazio, N. I., and Weitzman, M. D. (2010) The MRN complex in double-strand break repair and telomere maintenance. *FEBS Lett.* **584,** 3682–3695 CrossRef Medline
23. Paull, T. T., and Gellert, M. (1998) The 3′ to 5′ exonuclease activity of Mre 11 facilitates repair of DNA double-strand breaks. *Mol. Cell* **1,** 969–979 CrossRef Medline
24. Usui, T., Ohta, T., Oshiumi, H., Tomizawa, J., Ogawa, H., and Ogawa, T. (1998) Complex formation and functional versatility of Mre11 of budding yeast in recombination. *Cell* **95,** 705–716 CrossRef Medline
25. Furuse, M., Nagase, Y., Tsubouchi, H., Murakami-Murofushi, K., Shibata, T., and Ohta, K. (1998) Distinct roles of two separable *in vitro* activities of yeast Mre11 in mitotic and meiotic recombination. *EMBO J.* **17,** 6412–6425 CrossRef Medline
26. Symington, L. S., and Gautier, J. (2011) Double-strand break end resection and repair pathway choice. *Annu. Rev. Genet.* **45,** 247–271 CrossRef Medline
27. Hopfner, K. P., Karcher, A., Shin, D. S., Craig, L., Arthur, L. M., Carney, J. P., and Tainer, J. A. (2000) Structural biology of Rad50 ATPase: ATP-driven conformational control in DNA double-strand break repair and the ABC-ATPase superfamily. *Cell* **101,** 789–800 CrossRef Medline
28. Raymond, W. E., and Kleckner, N. (1993) RAD50 protein of *S. cerevisiae* exhibits ATP-dependent DNA binding. *Nucleic Acids Res.* **21,** 3851–3856 CrossRef Medline
29. Melby, T. E., Ciampaglio, C. N., Briscoe, G., and Erickson, H. P. (1998) The symmetrical structure of structural maintenance of chromosomes (SMC) and MukB proteins: long, antiparallel coiled coils, folded at a flexible hinge. *J. Cell Biol.* **142,** 1595–1604 CrossRef Medline
30. Walker, J. E., Saraste, M., Runswick, M. J., and Gay, N. J. (1982) Distantly related sequences in the α- and β-subunits of ATP synthase, myosin, kinases and other ATP-requiring enzymes and a common nucleotide binding fold. *EMBO J.* **1,** 945–951 CrossRef Medline
31. Hopfner, K. P., Craig, L., Moncalian, G., Zinkel, R. A., Usui, T., Owen, B. A., Karcher, A., Henderson, B., Bodmer, J. L., McMurray, C. T., Carney, J. P., Petrini, J. H., and Tainer, J. A. (2002) The Rad50 zinc-hook is a structure joining Mre11 complexes in DNA recombination and repair. *Nature* **418,** 562–566 CrossRef Medline
32. Lammens, K., Bemeleit, D. J., Möckel, C., Clausing, E., Schele, A., Hartung, S., Schiller, C. B., Lucas, M., Angermüller, C., Söding, J., Strässer, K., and Hopfner, K. P. (2011) The Mre11:Rad50 structure shows an ATP-dependent molecular clamp in DNA double-strand break repair. *Cell* **145,** 54–66 CrossRef Medline
33. Möckel, C., Lammens, K., Schele, A., and Hopfner, K. P. (2012) ATP driven structural changes of the bacterial Mre11:Rad50 catalytic head complex. *Nucleic Acids Res.* **40,** 914–927 CrossRef Medline
34. Anderson, D. E., Trujillo, K. M., Sung, P., and Erickson, H. P. (2001) Structure of the Rad50 x Mre11 DNA repair complex from *Saccharomyces cerevisiae* by electron microscopy. *J. Biol. Chem.* **276,** 37027–37033 CrossRef Medline
35. de Jager, M., van Noort, J., van Gent, D. C., Dekker, C., Kanaar, R., and Wyman, C. (2001) Human Rad50/Mre11 is a flexible complex that can tether DNA ends. *Mol. Cell* **8,** 1129–1135 CrossRef Medline
36. Hopfner, K. P., Karcher, A., Craig, L., Woo, T. T., Carney, J. P., and Tainer, J. A. (2001) Structural biochemistry and interaction architecture of the DNA double-strand break repair Mre11 nuclease and Rad50-ATPase. *Cell* **105,** 473–485 CrossRef Medline
37. Moreno-Herrero, F., de Jager, M., Dekker, N. H., Kanaar, R., Wyman, C., and Dekker, C. (2005) Mesoscale conformational changes in the DNA-repair complex Rad50/Mre11/Nbs1 upon binding DNA. *Nature* **437,** 440–443 CrossRef Medline
38. Paull, T. T. (2018) 20 Years of Mre11 biology: no end in sight. *Mol. Cell* **71,** 419–427 CrossRef Medline
39. Lau, W. C., Li, Y., Liu, Z., Gao, Y., Zhang, Q., and Huen, M. S. (2016) Structure of the human dimeric ATM kinase. *Cell Cycle* **15,** 1117–1124 CrossRef Medline
40. Reid, R. J., González-Barrera, S., Sunjevaric, I., Alvaro, D., Ciccone, S., Wagner, M., and Rothstein, R. (2011) Selective ploidy ablation, a high-throughput plasmid transfer protocol, identifies new genes affecting topoisomerase I-induced DNA damage. *Genome Res.* **21,** 477–486 CrossRef Medline
41. Brunn, G. J., Hudson, C. C., Sekulić, A., Williams, J. M., Hosoi, H., Houghton, P. J., Lawrence, J. C., Jr., and Abraham, R. T. (1997) Phosphorylation of the translational repressor PHAS-I by the mammalian target of rapamycin. *Science* **277,** 99–101 CrossRef Medline
42. Baroni, E., Viscardi, V., Cartagena-Lirola, H., Lucchini, G., and Longhese, M. P. (2004) The functions of budding yeast Sae2 in the DNA damage response require Mec1- and Tel1-dependent phosphorylation. *Mol. Cell. Biol.* **24,** 4151–4165 CrossRef Medline
43. Mimitou, E. P., and Symington, L. S. (2009) DNA end resection: many nucleases make light work. *DNA Repair* **8,** 983–995 CrossRef Medline
44. Lee, J. H., and Paull, T. T. (2005) ATM activation by DNA double-strand breaks through the Mre11-Rad50-Nbs1 complex. *Science* **308,** 551–554 CrossRef Medline
45. Majka, J., Niedziela-Majka, A., and Burgers, P. M. (2006) The checkpoint clamp activates Mec1 kinase during initiation of the DNA damage checkpoint. *Mol. Cell* **24,** 891–901 CrossRef Medline
46. Shiotani, B., and Zou, L. (2009) Single-stranded DNA orchestrates an ATM-to-ATR switch at DNA breaks. *Mol. Cell* **33,** 547–558 CrossRef Medline
47. Reginato, G., Cannavo, E., and Cejka, P. (2017) Physiological protein blocks direct the Mre11-Rad50-Xrs2 and Sae2 nuclease complex to initiate DNA end resection. *Genes Dev.* **31,** 2325–2330 CrossRef Medline
48. Trujillo, K. M., Yuan, S. S., Lee, E. Y., and Sung, P. (1998) Nuclease activities in a complex of human recombination and DNA repair factors Rad50, Mre11, and p95. *J. Biol. Chem.* **273,** 21447–21450 CrossRef Medline
49. Myler, L. R., Gallardo, I. F., Soniat, M. M., Deshpande, R. A., Gonzalez, X. B., Kim, Y., Paull, T. T., and Finkelstein, I. J. (2017) Single-molecule imaging reveals how Mre11-Rad50-Nbs1 initiates DNA break repair. *Mol. Cell* **67,** 891–898.e4 CrossRef Medline

50. Deshpande, R. A., Lee, J. H., and Paull, T. T. (2017) Rad50 ATPase activity is regulated by DNA ends and requires coordination of both active sites. *Nucleic Acids Res.* **45,** 5255–5268 CrossRef Medline
51. Chen, L., Trujillo, K. M., Van Komen, S., Roh, D. H., Krejci, L., Lewis, L. K., Resnick, M. A., Sung, P., and Tomkinson, A. E. (2005) Effect of amino acid substitutions in the rad50 ATP binding domain on DNA double strand break repair in yeast. *J. Biol. Chem.* **280,** 2620–2627 CrossRef Medline
52. van der Linden, E., Sanchez, H., Kinoshita, E., Kanaar, R., and Wyman, C. (2009) RAD50 and NBS1 form a stable complex functional in DNA binding and tethering. *Nucleic Acids Res.* **37,** 1580–1588 CrossRef Medline
53. Paull, T. T. (2015) Mechanisms of ATM Activation. *Annu. Rev. Biochem.* **84,** 711–738 CrossRef Medline
54. Lee, J. H., Mand, M. R., Deshpande, R. A., Kinoshita, E., Yang, S. H., Wyman, C., and Paull, T. T. (2013) Ataxia telangiectasia-mutated (ATM) kinase activity is regulated by ATP-driven conformational changes in the Mre11/Rad50/Nbs1 (MRN) complex. *J. Biol. Chem.* **288,** 12840–12851 CrossRef Medline
55. Bakkenist, C. J., and Kastan, M. B. (2003) DNA damage activates ATM through intermolecular autophosphorylation and dimer dissociation. *Nature* **421,** 499–506 CrossRef Medline
56. Sun, Y., Jiang, X., Chen, S., Fernandes, N., and Price, B. D. (2005) A role for the Tip60 histone acetyltransferase in the acetylation and activation of ATM. *Proc. Natl. Acad. Sci. U.S.A.* **102,** 13182–13187 CrossRef Medline
57. Pellegrini, M., Celeste, A., Difilippantonio, S., Guo, R., Wang, W., Feigenbaum, L., and Nussenzweig, A. (2006) Autophosphorylation at serine 1987 is dispensable for murine Atm activation *in vivo*. *Nature* **443,** 222–225 CrossRef Medline
58. Osley, M. A., and Shen, X. (2006) Altering nucleosomes during DNA double-strand break repair in yeast. *Trends Genet.* **22,** 671–677 CrossRef Medline
59. Tsukuda, T., Fleming, A. B., Nickoloff, J. A., and Osley, M. A. (2005) Chromatin remodelling at a DNA double-strand break site in *Saccharomyces cerevisiae*. *Nature* **438,** 379–383 CrossRef Medline
60. Stracker, T. H., and Petrini, J. H. (2011) The MRE11 complex: starting from the ends. *Nat. Rev. Mol. Cell Biol.* **12,** 90–103 CrossRef Medline
61. Cassani, C., Vertemara, J., Bassani, M., Marsella, A., Tisi, R., Zampella, G., and Longhese, M. P. (2019) The ATP-bound conformation of the Mre11-Rad50 complex is essential for Tel1/ATM activation. *Nucleic Acids Res.* **47,** 3550–3567 CrossRef Medline
62. Oh, J., Al-Zain, A., Cannavo, E., Cejka, P., and Symington, L. S. (2016) Xrs2 dependent and independent functions of the Mre11-Rad50 complex. *Mol. Cell* **64,** 405–415 CrossRef Medline
63. Wanrooij, P. H., Tannous, E., Kumar, S., Navadgi-Patil, V. M., and Burgers, P. M. (2016) Probing the Mec1ATR checkpoint activation mechanism with small peptides. *J. Biol. Chem.* **291,** 393–401 CrossRef Medline
64. Poltoratsky, V. P., Shi, X., York, J. D., Lieber, M. R., and Carter, T. H. (1995) Human DNA-activated protein kinase (DNA-PK) is homologous to phosphatidylinositol kinases. *J. Immunol.* **155,** 4529–4533 Medline
65. Trujillo, K. M., and Sung, P. (2001) DNA structure-specific nuclease activities in the *Saccharomyces cerevisiae* Rad50*Mre11 complex. *J. Biol. Chem.* **276,** 35458–35464 CrossRef Medline
66. Bylund, G. O., Majka, J., and Burgers, P. M. (2006) Overproduction and purification of RFC-related clamp loaders and PCNA-related clamps from *Saccharomyces cerevisiae*. *Methods Enzymol.* **409,** 1–11 CrossRef Medline
67. Gomes, X. V., Schmidt, S. L., and Burgers, P. M. (2001) ATP utilization by yeast replication factor C. II. Multiple stepwise ATP binding events are required to load proliferating cell nuclear antigen onto primed DNA. *J. Biol. Chem.* **276,** 34776–34783 CrossRef Medline

Activation of Tel1^{ATM} kinase requires Rad50 ATPase and long nucleosome-free DNA but no DNA ends

Sarem Hailemariam, Sandeep Kumar and Peter M. Burgers

J. Biol. Chem. 2019, 294:10120-10130.
doi: 10.1074/jbc.RA119.008410 originally published online May 9, 2019

Supporting information to:

Activation of Tel1^{ATM} kinase requires Rad50 ATPase and long nucleosome-free DNA, but no DNA ends

Sarem Hailemariam[1], Sandeep Kumar[1,2], and Peter M. Burgers[1]*

[1]Department of Biochemistry and Molecular Biophysics, Washington University School of Medicine, Saint Louis, Missouri, USA, [2]current address: Intellia Therapeutics, Cambridge, MA 02139.

*Corresponding author: TEL (314) 362-3772; FAX (314) 362-7183; burgers@wustl.edu

---

DNA substrates used:

20mer: 5'-TTGATAAGAGGTCATTTTT
40mer: 5'-TTGATAAGAGGTCATTTTTGCGGATGGCTTAGAGCTTAAT
60mer: 5'-ACATGTTGAGCTACAGCACCAGATTCAGCAATTAAGCTCTAAGCCATCCGCAAAAATGAC
80mer: 5'-TTGATAAGAGGTCATTTTTGCGGATGGCTTAGAGCTTAATTGCTGAATCTGGTGCTGTAG
CTCAACATGTTTTAAATATG
147mer: 5'-ATCGAGAATCCCGGTGCCGAGGCCGCTCAATTGGTCGTAGACAGCTCTAGCACCGCTTA
AACGCACGTACGCGCTGTCCCCCGCGTTTTAACCGCCAAGGGGATTACTCCCTAGTCTCCAGG
CACGTGTCAGATATATACATCCGAT

Oligonucleotides were hybridized to their complementary sequences in a 1:1 ratio to form blunt-end dsDNAs. The sequence of the 80-mer shown was used as ssDNA in the experiment shown in Fig. 3A. The 147-mer sequence is the Widom 601 sequence (1), and was purchased from EpiCypher, as was the mononucleosome assembled on the same sequence, and used in Fig. 4B,C.

1. Lowary, P.T., and Widom, J. (1998). New DNA sequence rules for high affinity binding to histone octamer and sequence-directed nucleosome positioning. J Mol Biol *276*, 19-42.

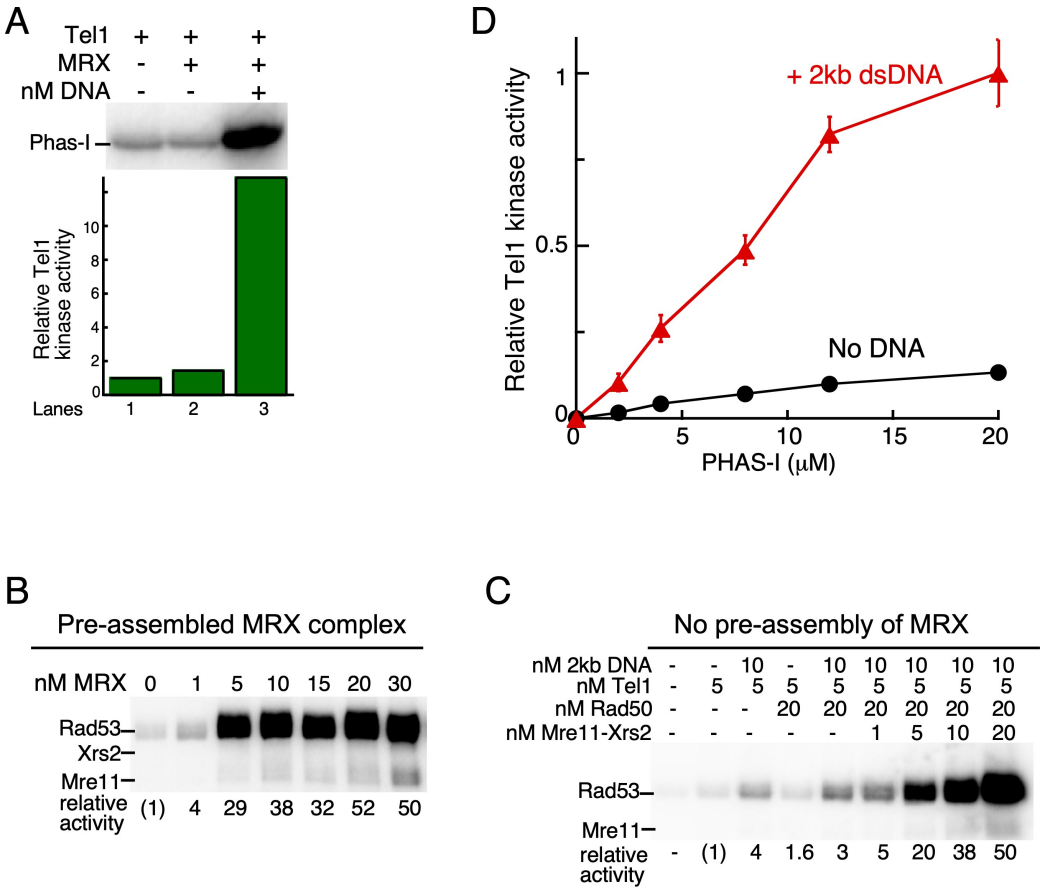

FIGURE S1. **Tel1 activation by MRX and DNA.** *A*, standard kinase reactions contained 2 μM PHAS-I and 50 μM [γ-^{32}P]-ATP in kinase buffer with or without 30 nM MRX and 5 nM 2 kb linear DNA. Kinase reactions were initiated with 5 nM Tel1. Reactions analyzed by 15% SDS-PAGE, followed by phosphorimaging. A representative experiment is shown at top. Bottom, phosphorylation of PHAS-I was quantified and plotted as fold increase of Tel1 kinase activity with lane 1 set at 1. The migration of PHAS-I (15 kDa) is as shown. *B,* standard kinase reactions contained 5 nM Tel1, 10 nM 2kb linear DNA, 200 nM Rad53, and the indicated concentrations of MRX. The MRX used in this experiment was pre-assembled by incubating 300 nM Rad50 with 300 nM Mre11-Xrs2 at 0 ˚C for one hour, prior to dilution into the assay. Rad53 phosphorylation was quantified by setting Tel1 alone reaction (lane 1) to 1. *C*, kinase reactions contained 5 nM Tel1, 10 nM 2kb linear DNA, 200 nM Rad53, 20 nM Rad50. The indicated concentrations of Mre11-Xrs2 was added into the assay at 0 ˚C and the assay incubated at 30 ˚C for 15 min. Rad53 phosphorylation was quantified by setting Tel1 alone reaction (lane 2) to 1. *D,* standard kinase reactions contained 5 nM Tel1, 30 nM MRX, and increasing concentrations of PHAS-I in the presence or absence of 5 nM 2kb linear DNA. In panels B and C the migration of GST-Rad53-kd (118 kDa), Xrs2 (96 kDa), and Mre11 (77 kDa) is as shown.

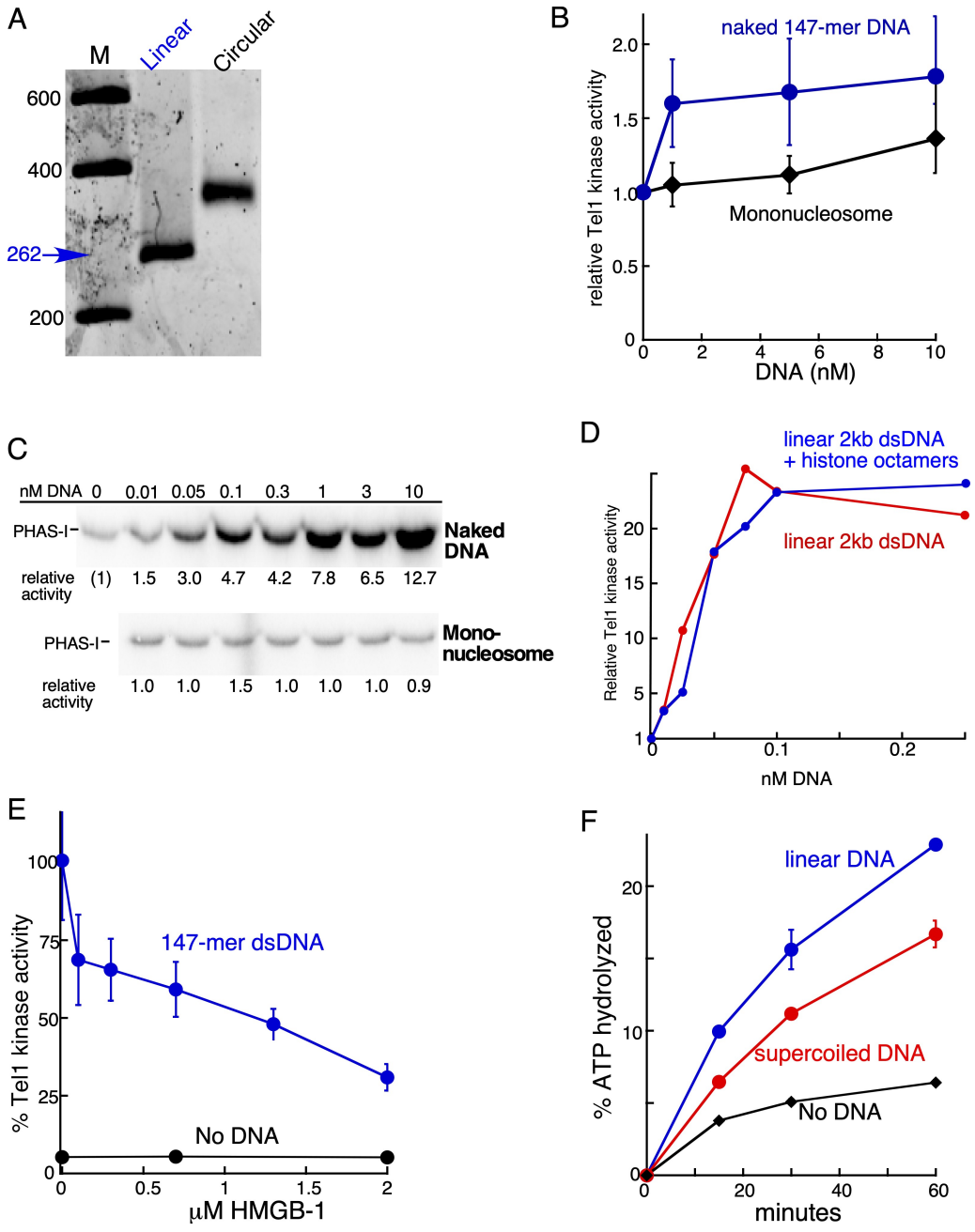

FIGURE S2. **Nucleosome-free DNA, but not DNA ends, is required for Tel1 activation.** *A, preparation of 262-mer circular DNA.* A 262-mer DNA fragment was cut out of a 3 kb plasmid by *Sal*1 and *Xho*1 digestion, and purified by differential PEG_{8000} precipitation in 0.5 M NaCl. The 5-9% w/w cut was >90% pure. It was ligated in a 1 ml ligation reaction containing 20 mM Tris-HCl 7.6, 100 mM Na-acetate, 10 mM Mg-acetate, 1 mM ATP, 1 mM spermidine, 1.5 μg/ml ethidium bromide, 50 nM 262-mer fragment, and 4,000 units of T4 ligase, for 24 h at 13 ˚C. The optimal concentration of ethidium bromide to obtain circularization was previously determined in a test assay with concentrations varying between 0.2-10 μg/ml. The DNA was recovered by ethanol precipitation, and the circular DNA was purified on a 3% preparative Metaphor gel. The

linear DNA was purified on the same gel to remove contaminating plasmid DNA. A comparison of the linear and circular preparations is shown on a 3% Metaphor gel, which was stained with GelRed. *B, Tel1 alone is not stimulated by nucleosomal DNA.* Standard kinase reactions without MRX contained 5 nM Tel1, and increasing concentrations of either 147 bp naked DNA, or the nucleosome assembled on the same DNA. Phosphorylation of Rad53-kd was quantified as fold increase of Tel1 kinase activity, with no DNA set to 1. *C, nucleosomal DNA does not stimulate Tel1 in the MRX-dependent assay using PHAS-I as substrate.* Standard kinase reactions lacking contained 5 nM Tel1, 30 nM MRX, 2 μM PHAS-I instead of Rad53-kd, and increasing concentrations of either 147 bp naked DNA, or the nucleosome assembled on the same DNA. Phosphorylation of PHAS-I was quantified as fold increase of Tel1 kinase activity with lane 1 (on naked DNA gel) set at 1. The migration of PHAS-I (15 kDa) is as shown. *D, free histone octamers do not inhibit Tel1 kinase.* Standard kinase reactions contained 5 nM Tel1, 30 nM MRX, 200 nM Rad53, and increasing concentrations of 2 kb linear DNA with or without increasing concentrations of histone octamers. The concentration of histone octamers required to coat DNA was calculated for each DNA concentration with a single octamer wrapping 147 bp. Relative Tel1 activity was calculated by setting the reaction without DNA to 1. *E, DNA coating by HMGB-1 inhibits Tel1.* Standard kinase reactions contained 5 nM Tel1, 30 nM MRX, 200 nM Rad53-kd, either no DNA or 1 nM 147-mer dsDNA, as indicated, and increasing concentrations of HMGB-1. *F, ATPase activity of MRX is stimulated preferentially by linear DNA.* Standard ATPase reactions contained 50 μM [γ-^{32}P]-ATP, 100 nM MRX, and 1 nM of the indicated 2 kb DNA. Radioactive ATP and ADP were separated by PEI-Cellulose TLC and quantified as described (1).

1. Chen, L., Trujillo, K. M., Van Komen, S., Roh, D. H., Krejci, L., Lewis, L. K., Resnick, M. A., Sung, P., and Tomkinson, A. E. (2005) Effect of amino acid substitutions in the rad50 ATP binding domain on DNA double strand break repair in yeast. *J Biol Chem* **280**, 2620-2627

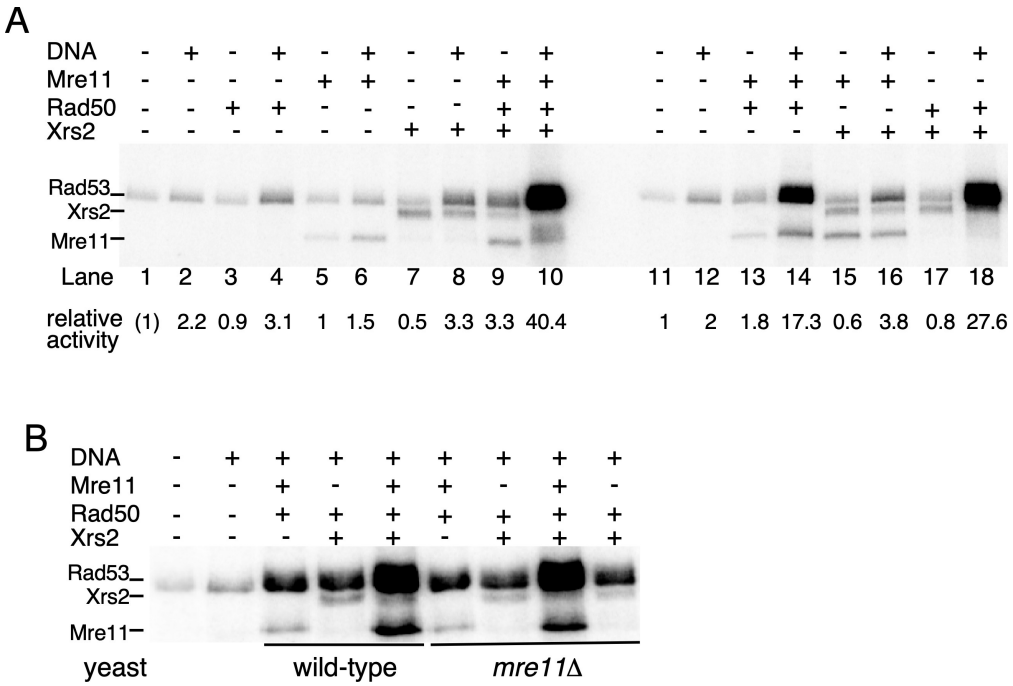

FIGURE S3. *A*, **Single subunits of MRX do not show a substantial activation of Tel1 kinase**. *A*, standard kinase reaction with 5 nM Tel1, 200 nM Rad53, and 30 nM Mre11, Rad50, or Xrs2, with or without 5 nM linear 2 kb DNA (left panel, lanes 1-8). The right panel (lanes 9-18) is the same data presented in FIGURE 5A. Lanes 9 and 10 of the left panel are presented as lanes 9 and 10 in Fig. 5A. Relative Tel1 kinase activity was calculated by setting Tel1 alone (lane 1) to 1. *B*, standard kinase reaction with 5 nM Tel1, 200 nM Rad53, and 30 nM MR, RX or MRX, with 5 nM linear 2 kb DNA. The Rad50 protein used in lanes 3-5 is purified from a wild-type yeast strain while the Rad50 used in the last four lanes is from a yeast *mre11Δ* strain. In all panels, the migration of GST-Rad53-kd (118 kDa), Xrs2 (96 kDa), and Mre11 (77 kDa) is as shown.